Plan Shear Indicator for Real-Time Doppler Radar Identification of Hazardous Storm Winds

GRAHAM M. ARMSTRONG AND RALPH J. DONALDSON, JR.

Air Force Cambridge Research Laboratories, Sudbury, Mass.

(Manuscript received 10 December 1968, in revised form 12 March 1969)

ABSTRACT

The Plan Shear Indicator (PSI) is a new mode for display of meteorological Doppler radar information which may prove to be valuable in identification of hazardous winds and turbulence in storms. It provides real-time location and convenient highlighting of regions within precipitation echoes of abnormally large shear and spectral broadening of the Doppler velocity. The real-time capability of the PSI and its high data rate are achieved at the cost of mediocre resolution of ranges and velocities, and the ability to display only the shear and not the absolute value of wind components along the Doppler beam.

The PSI display for a scanning Doppler radar utilizes an ordinary PPI scope intensity-modulated by a coherent memory filter. The resultant pattern is a series of concentric arcs, each one located on the scope at its appropriate range plus an incremental displacement which depends on the radial component of velocity at that range. Radial shear is indicated by gaps or bunching of the arcs, while tangential shear, as, for example, a vortex, is indicated by wrinkles in the arcs. Turbulence on a scale smaller than measurable wind shear would broaden the Doppler spectrum and would be revealed on the PSI by an increase in line widths of the arcs. The instrument has been used during an outbreak of severe thunderstorms in New England, and appeared to be successful in identification of storms which produced damaging winds and hail.

1. Introduction

Wind measurement by Doppler radar is dependent on a medium which can trace the air motion reliably and, at the same time, scatter sufficient power back to the radar to provide a detectable signal. These requirements are satisfied by the precipitation in a storm, for determination of the component of mean wind velocity along the radar beam, on a scale of resolution attainable by meteorological radars.

The employment of Doppler radar for measurement of winds in a tornado was first reported by Smith and Holmes (1961). Using a cw Doppler without ranging capability, they observed Doppler shifts corresponding to wind speeds up to 200 mph when the radar was directed toward a tornado which devasted El Dorado, Kan., on 10 June 1958. The use of pulse Doppler radar with range-velocity display was suggested by Lhermitte (1964) for detection of a vortex. Although no pulse Doppler data had been acquired in a high-speed vortex such as a tornado, Lhermitte derived the characteristic patterns which would be revealed by vortices both larger and smaller than the resolution of the radar beam and ranging circuitry. Neither of these schemes, however, provided the convenience of a map-like presentation of dangerous wind speeds in real time.

A compromise solution is offered by the Plan Shear Indicator, or PSI, developed by the authors (1968) for use with the AFCRL meteorological Doppler radar at Sudbury, Mass. This technique converts an inherent limitation—mediocre range resolution—into an advantage by utilizing the distance between adjacent range elements as a field for presentation of velocity. The velocity information is obtained in real time from a coherent memory filter which performs a frequency analysis at all ranges of the Doppler signal returned by precipitation or detectable cloud. The display of the coherent memory filter output on an ordinary PPI scope, as the Doppler radar scans in azimuth, provides a pattern in which regions of intense wind shear or turbulence may be located with ease and readily distinguished from a homogeneous wind field. Although the *magnitude* of the wind cannot be measured quantitatively in this manner, the PSI technique is a sensitive probe of the radial component of the *gradient* of the wind in space, or wind shear. The technique has a potential application as an aid to flight safety because wind shears within precipitation which are hazardous to aircraft may be recognized immediately. Furthermore, a vortex circulation of sufficient scale to be resolved by the radar has a characteristic signature on the PSI display which may be of use in identification and warning of severe thunderstorm events at the surface.

2. Velocity determination by the coherent memory filter

Frequency analysis of the received echo signal is a basic requirement for full utilization of the information

provided by pulse Doppler radar. Methods for producing accurate, detailed spectra at the same speed at which information is acquired have been restricted to analyses of single range elements, although recent advances in fast Fourier transform techniques offer promise for significant improvements. However, an instrument has been developed during the past decade for providing coarse but real-time Doppler spectral analysis over the entire range capability of the radar. This circuit is called a Coherent Memory Filter (CMF) or sometimes a Velocity Indicating Coherent Integrator (VICI). Chimera (1960) first recognized the possibilities for application of the CMF to meteorological analysis. A concise description of the CMF and an illustration of its use by Chimera in a snowstorm have been presented in an excellent review article on radar meteorology by Atlas (1963).

The following explanation of the operation of the CMF should be sufficient for understanding the principles of its use in measurement of velocities. However, a more comprehensive discussion and mathematical treatment of the CMF is available in a survey article by Groginsky (1965), which also lists references to the basic development work by Bickel *et al.* (1959) and others.

The signal which is scattered back from a fixed target exhibits a constant phase difference ϕ with respect to the transmitter signal phase. This phase difference, given by

$$\phi = 4\pi r/\lambda, \tag{1}$$

is merely the time required for radar energy of wavelength λ to reach the target at range r, and return, expressed as a multiple of the time required for one oscillation of the radar transmitter. In Doppler radar, provision is made for measuring the phase difference of the returned signal within the limits of 0 to 2π. If the range of the target changes, the phase difference ϕ also changes and becomes a function of time. A change in phase with respect to time is an angular speed $2\pi f_d$; therefore, time differentiation of (1) yields

$$f_d = 2v_r/\lambda, \tag{2}$$

where f_d is the Doppler frequency shift and v_r is the radial velocity of the target.

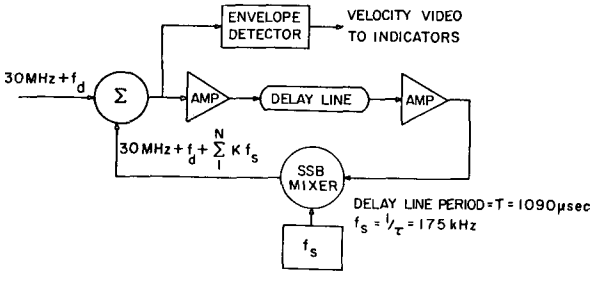

FIG. 1. Simplified block diagram of the Coherent Memory Filter.

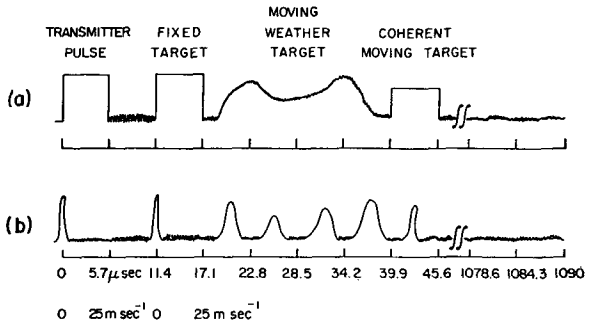

FIG. 2. Typical "A" scope display of radar video, (a), and corresponding display of Coherent Memory Filter output video, (b). Note the velocity interval of 0–25 m sec^{-1} every 5.7 μsec. Fixed targets appear at zero velocity while moving targets appear somewhere in the velocity interval depending upon their radial velocity component.

The CMF, as shown in Fig. 1, consists simply of a summing network, Σ, a delay line and associated amplifiers, a single sideband mixer, a frequency generator which produces a frequency whose period matches the radar pulse width τ, and an envelope detector. If we neglect the single sideband mixer for a moment and circulate a series of N pulses from a stationary target through a delay line whose delay time equals the pulse repetition interval T, and then add them together in the summing network, they will produce an output with a peak N times as great as the amplitude of the individual pulse.

It is obvious from (1) that successive pulses from moving targets delayed by T will not be in phase and will not add directly. If moving targets are to be detected, the phase of successive pulses must be shifted somewhere between 0 and 2π radians during the time of each pulse width τ, so as to achieve the correct phase relationship to add coherently during some portion of the time a particular pulse is present in the summing network. A linear time-varying phase shift is equivalent to a frequency shift. Accordingly, the phase shifter can be replaced by a scanning frequency f_s with a period equal to the pulse width τ (i.e., $f_s = 1/\tau$) and a single sideband mixer whose output frequency is the sum of the input frequency and the scanning frequency f_s. Since the CMF works in the i.f. region, a simple envelope detector is needed to produce the output video.

The output signal of the AFCRL CMF, illustrated in Fig. 2b, is a series of 192 range bins each with a period $\tau = 5.7$ μsec. This gives a range resolution of 855 m and a total range of 164 km. The Doppler spectrum of the target(s) within each of the range bins is displayed with zero velocity at the left of the range bin. Increasing radial velocity (toward the radar) is indicated by an increasing displacement toward the right. In the case of a pulse Doppler radar the phase change ϕ is measured only at discrete time intervals T, equal to the pulse repetition period. Since the CMF is incapable of detecting phase shifts greater than 2π, velocities can be

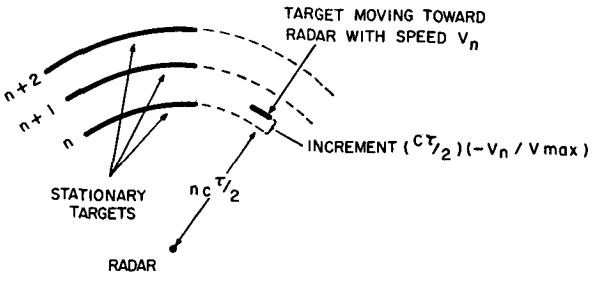

FIG. 3. PSI display for stationary targets (left) and a moving target (right). The moving target is located at the same distance from the radar as the nearest stationary target, but is displaced from it on the PSI display by an increment which depends on its velocity.

measured unambiguously only if the target range changes less than a distance $\lambda/2$ during the period T. In our CMF, $T=1090\ \mu$sec and $\lambda=5.45$ cm, so maximum unambiguous velocity or $v_{max}=\lambda/2T=25$ m sec^{-1}.

The pulses are amplitude-weighted, as they are circulated through the delay line, in order to enhance the velocity resolution of the CMF. Each time a pulse is circulated through the delay line, it is stepped up in frequency by an amount f_s. After 20 circulations the pulse amplitude has reached a peak, and at circulations 10 and 30 the pulses attain approximately half their peak amplitude.

If a PPI scope with a fast enough sweep speed to resolve the range bins is intensity-modulated by the output of the CMF, as illustrated in Fig. 2b, a series of concentric arcs will mark the location of targets as the antenna is rotated in azimuth. We call this display a Plan Shear Indicator or PSI because of its capability to detect and locate regions of strong wind shear from the characteristics of the arc pattern.

3. Interpretation of Plan Shear Indicator patterns

The indicated range r_n of an arc on the PSI display is the sum of the true distance of the range element in which the target is detected, plus an incremental displacement, no greater than the width of a range element, which corresponds to the radial velocity of the target; thus,

$$r_n=(c\tau/2)(n-v_n/v_{max}), \tag{3}$$

where c is the speed of electromagnetic propagation, τ the radar pulse duration, and $\tau/2$ the time interval required for the radar waves to traverse the width of a range element; n is an integer between 1 and T/τ which denotes the number of range elements between radar and target; $v_{max}=\lambda/2T$ is the maximum velocity which can be detected unambiguously by the radar; and v_n is the indicated radial velocity. Velocities are considered positive for motions directed away from the radar. Hence a target motion toward the radar will increase r_n as illustrated in Fig. 3.

The true radial velocity of the target will not be indicated correctly if it is positive, or if it is negative (toward the radar) with a magnitude in excess of v_{max}. During the pulse repetition period T the Doppler radar can detect phase changes only within 0 to 2π, corresponding to $0\leq -v_n\leq v_{max}$. Velocity ambiguity will occur if the true radial velocity exceeds this range, and the indicated radial velocity v_n will then express the remainder after the true velocity is reduced by an integral multiple of v_{max} until $0\leq -v_n\leq v_{max}$. For example, if $v_{max}=25$ m sec^{-1} and a target is moving toward the radar at a speed of 60 m sec^{-1}, its indicated velocity will be 10 m sec^{-1}. Another target retreating from the radar at a speed of 20 m sec^{-1} will be indicated the same as a target moving toward the radar at 5 m sec^{-1}.

Note that the two terms of r_n in (3) differ considerably in magnitude. The increment corresponding to velocity, $(c\tau/2)$ $(-v_n/v_{max})$, is generally very small compared with the target range $nc\tau/2$. Therefore, the PSI display cannot be used to measure velocities with acceptable accuracy. However, *changes* in velocity from one range element to the next one, or along a single range element as the antenna scans, are easily detectable and may be evaluated without great difficulty. As the radar antenna rotates, the PSI presents a series of up to T/τ concentric arcs. The number and size of the arcs depends on the area of target which is detected. If the radial velocity were constant, as in observation of fixed ground targets, the arcs would be circular and evenly spaced. If, however, there is a gradient of the radial velocities of the detected targets along the radial direction (i.e., radial shear), the spacing between arcs would vary. Similarly, if a gradient of the radial velocities exists normal to the radar beam (i.e., tangential shear), the radius of an arc will vary with azimuth as the antenna scans, and the PSI display will have wiggles in it.

Consider first the significance of arc spacing in the PSI pattern. At a fixed azimuth angle, the indicated distance Δr between two successive arcs n and $n+1$ is given from (3) as

$$\Delta r=r_{n+1}-r_n=(c\tau/2)[1-(v_{n+1}-v_n)/v_{max}]. \tag{4}$$

Substituting $\lambda/2T$ for v_{max}, we can express the change in velocity $\Delta v=v_{n+1}-v_n$ by

$$\Delta v=(c\tau/2-\Delta r)(\lambda/c\tau T). \tag{5}$$

If the y axis of Cartesian coordinates is assumed to be identical with the direction in which the radar antenna points, the true range Δy between adjacent arcs is $c\tau/2$, and the radial shear of the radial wind component is given by dividing (5) by Δy, i.e.,

$$\Delta v/\Delta y=(1-2\Delta r/c\tau)(\lambda/c\tau T). \tag{6}$$

The maximum value of $\Delta v/\Delta y$ which can be measured unambiguously is $\lambda/(c\tau T)$, which would be the case if

$\Delta v = v_{max}$ and $\Delta r = 0$. With our particular radar and CMF, $\lambda = 5.45$ cm, $\tau = 5.7$ μsec and $T = 1090$ μsec; thus, $\lambda/(c\tau T) = 2.9 \times 10^{-2}$ sec^{-1}. If Δv is positive but less than v_{max}, Δr will be smaller than the width of a range element. Positive Δv means that the air motion away from the radar increases with distance. Consequently, the bunching-up of arcs on the PSI display indicates a divergent radial component of the wind and, conversely, a larger than normal gap between arcs indicates a convergent radial component of air motion. If $|\Delta v| > v_{max}$, one or both of the velocities is ambiguously recorded, and the resultant arc spacing cannot be interpreted without examination of the continuity of airflow in surrounding areas.

Abnormal spectral broadening is indicated by thickening of a PSI arc. Unfortunately, the width of the CMF output signal, which controls the thickness of the PSI arcs, is a function of received power as well as the width of the Doppler velocity spectrum. On the other hand, extremely wide arcs which fill up practically all of a range bin almost certainly reveal regions with a very large variance of the Doppler velocity spectrum, which is suggestive, if not indicative, of turbulence of sufficient intensity to constitute a hazard to aircraft (Donaldson and Wexler, 1969).

Now let us interpret the meaning of wiggles in a PSI arc. The slope of an arc at indicated range r_n with respect to the scanning radar beam is $dr_n/(r_n d\beta)$, where β is azimuth angle of the radar beam increasing with clockwise rotation. This slope may be evaluated in terms of tangential shear of the radial velocity by differentiating (3) with respect to the velocity v_n and substituting $\lambda/2T$ for v_{max} to obtain

$$dr_n/dv_n = -c\tau T/\lambda. \tag{7}$$

Tangential shear of radial velocity is defined by dv/dx in Cartesian coordinates, adopting the convention that the radar points in the y direction. In polar coordinates appropriate to a scanning radar, $dx = y d\beta$. Now on the PSI display true range y_n $(= nc\tau/2)$ does not equal indicated range r_n, unless $v_n = 0$ or an integral multiple of v_{max}. However, the maximum fractional error in approximating $y_n \approx r_n$ is $1/n$. (This occurs when $-v_n = v_{max}$.) The average error would be half as large. Since the velocity resolution of the CMF is no better than 2.5%, the approximation $y_n \approx r_n$ is completely acceptable for any $n > 20$, or true range of 17 km or more. Even at a range of 10 km the error is less than 5%. Therefore, tangential shear may be evaluated directly from the slope of the arc with respect to a circle by using (7) and the approximation $y_n \approx r_n$:

$$dv_n/dx = dv_n/y_n d\beta \approx -(\lambda/c\tau T) dr_n/r_n d\beta. \tag{8}$$

Note that tangential shear as defined above is the first of the two terms, $dv/dx - du/dy$, which express vorticity in Cartesian coordinates. Accordingly, positive tangential shear, indicated on the PSI display by slope of an arc toward the radar, moving clockwise, contributes toward positive or cyclonic vorticity. If an arc tilts 45° from a constant velocity circular path, the magnitude of the shear will be $\lambda/(c\tau T)$, or 2.9×10^{-2} sec^{-1} with our equipment.

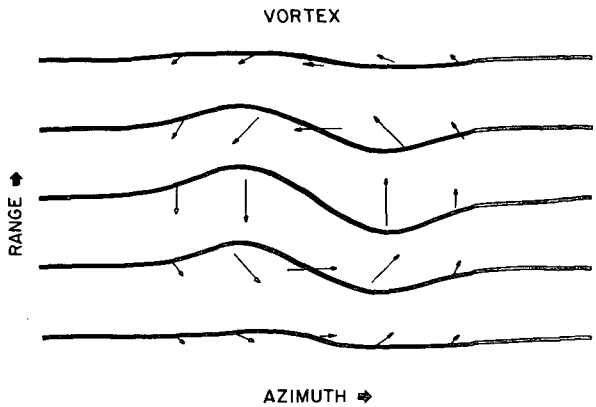

FIG. 4. Schematic PSI pattern for a cyclonic vortex. Arrows represent wind vectors. Maximum vorticity is denoted by maximum arc slope, in the center of the sketch.

The maximum value of tangential shear which can be measured unambiguously occurs when the breadth of the unambiguous velocity spectrum is not quite filled with contributions from both sides of the radar antenna beam. It is difficult to state the effective antenna aperture for detection of velocities, because this depends to a great extent on received power levels and sensitivity of the radar receiver. It is almost certainly greater than the traditional half-power beam width but unlikely to exceed twice this size. Our Doppler radar antenna has a half-power beam width of 0.9° with v_{max} of our coherent memory filter being 25 m sec^{-1}. Therefore, the maximum tangential shear which can be measured with our equipment is in the neighborhood of $0.8/r$ to $1.6/r$ sec^{-1}, where r is range in km.

Another possible limitation on the angular resolution of the PSI is the antenna scanning rate. The output powers of the CMF delay line weighting function exceed one-fourth of the maximum power during 20 pulse repetition periods, or $20 \times 1090 = 21{,}800$ μsec. If the antenna scans through one half-power beam width in this time (0.9°/0.0218 sec or 7 rpm), the CMF delay line will limit the angular resolution to the same extent as the antenna. Generally the antenna scans at a rate of 5 rpm, somewhat less than the rate at which the CMF delay line would have an appreciable effect on angular resolution. However, the CMF output peak amplitude is delayed by 20 recirculations in the delay line, or $20T = 0.0218$ sec. Consequently, at a normal antenna scanning rate of 5 rpm, the PSI pattern will be rotated about $\frac{2}{3}$ of a degree in the direction of antenna scan.

The most easily distinguished pattern feature on the PSI display is the contrast between areas of little or no

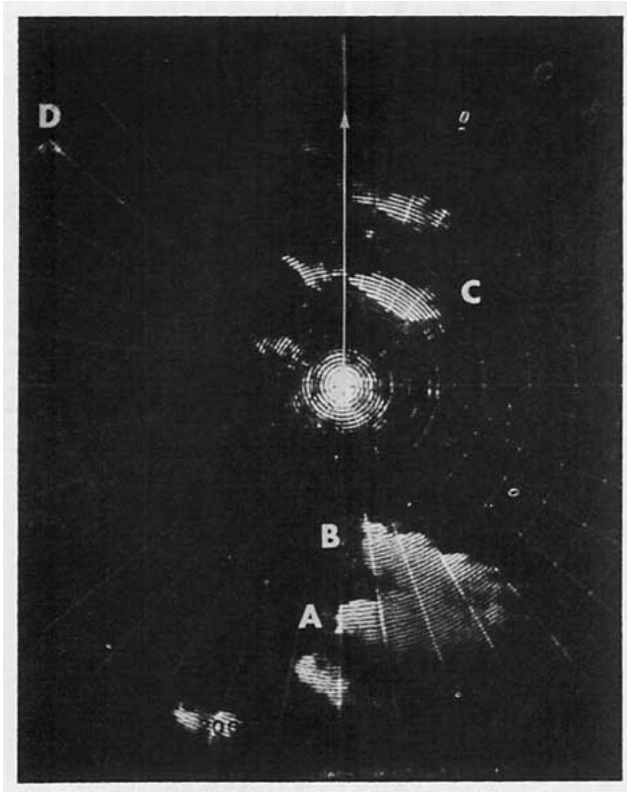

FIG. 5. Photograph of PSI display. This photograph and all of the succeeding ones (Figs. 6–10) were taken on 9 August 1968 from the AFCRL meteorological radar site at Sudbury, Mass., and show north at the top of the picture with 5-mi range markers in an eastern sector. Antenna elevation is 2°, time is 1352 EST. Letters A, B, C and D designate severe thunderstorms described in text.

wind shear, where the arcs are smooth and evenly spaced, and regions of intense shear in which the arcs exhibit a disturbed and sometimes confused appearance. The interpretation of a complex tangle of arcs, beyond the recognition that severe wind shear and turbulence is present, may be extremely difficult because 1) only the radial component of wind can be observed by Doppler radar, and only when suitable tracers are present; 2) careful inspection is required to circumvent the ambiguity of velocities which exceed the maximum unambiguous range; and 3) sometimes regions of large shear are also regions of broad velocity spectra which produce arc segments so thick that the boundaries between them are ill-defined. Nevertheless, some simple types of air circulation are revealed by a characteristic PSI pattern. For example, a wind-shift line with relatively smooth air on either side would show up on the PSI display as a locus of wrinkled arcs cutting across an otherwise undisturbed pattern. The PSI pattern for convergent flow or a sink would have the largest gaps in the arcs where convergence was greatest. A cyclonic vortex would have the pattern type sketched in Fig. 4, with the center of maximum vorticity indicated by the maximum clockwise slope of an arc toward the radar. We must caution, however, that the appearance of a pattern on a PSI display is no guarantee of the existence of the air-flow model corresponding with these examples, because a single Doppler radar can sense only the radial component of the total wind vector.

4. Application of Plan Shear Indicator to severe storm identification

Wind shear information has been acquired in a variety of convective storms, using the PSI display. Armstrong and Donaldson (1968) showed an example of an ordinary thunderstorm, in which no high winds or hailstones were reported, which occurred during the summer of 1967 near the AFCRL Doppler radar site at Sudbury, Mass. A few places in this storm showed minor wrinkles in the PSI arcs, indicating moderate shear.

The most interesting set of storms observed to date with the PSI display occurred on 9 August 1968. Several of the widely scattered thunderstorms observed on this day were severely damaging. Within range of the PSI display one storm released a small tornado and 1-inch hail; a second one nearby was not confirmed as a tornado but caused heavy wind damage with hail nearly 1 inch in diameter; a third storm struck a harbor inflicting extensive and heavy wind damage to small boats, also releasing marble-size hail; and a fourth

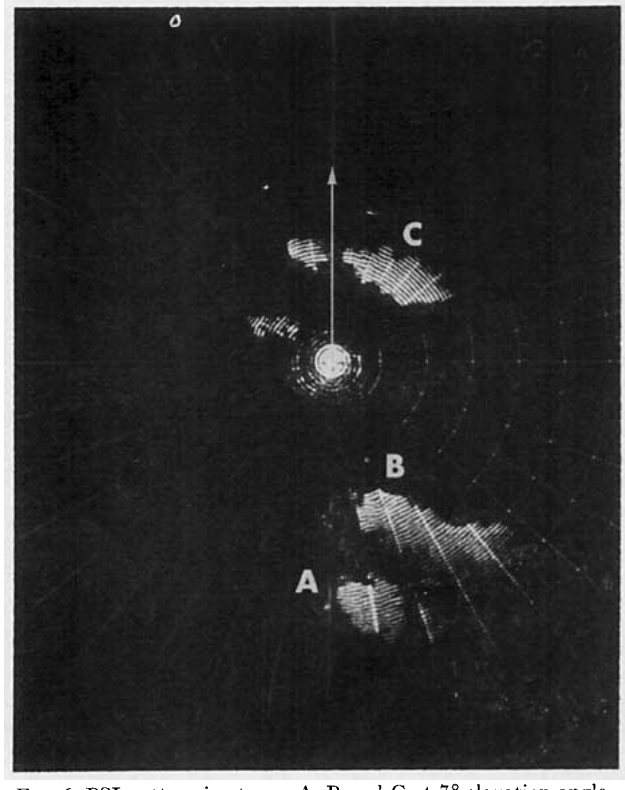

FIG. 6. PSI pattern in storms A, B and C at 7° elevation angle, 1353 EST. Note irregularities in PSI arcs in storms A and B.

storm deposited hail up to 2 inches in diameter but was accompanied by only minor wind damage. We shall label these storms A, B, C and D, respectively, for convenience in describing them.

In all four severe storms, disturbances occurred in the PSI pattern aloft for periods of 15 min to 1 hour before damaging winds or hail reached the ground. The storm A tornado and storm B episode of heavy wind damage both occurred around 1405–1410 EST. Fig. 5, some 10–15 min earlier, shows a relatively undisturbed low-level PSI pattern in all storms; but Fig. 6, photographed a minute after Fig. 5 with the antenna elevated 7°, shows a broad area of shear covering western parts of storms A and B at heights of about 5 and 3 km, respectively, in contrast to the more regular pattern of storm C. A few minutes later (Fig. 7, elevation 2°) there is a confused shear line just under 2 km in the incipient tornado of storm A and sharp wiggles at the 1-km level in a couple of the arcs of storm B. However, storm C, which did not release severe surface gusts until more than an hour later, still displays a smooth arc pattern.

A PSI pattern suggestive of a cyclonic vortex, as sketched in Fig. 4, appeared aloft in storm C about an hour before this storm caused severe wind damage, and persisted for most of this period. Fig. 8 shows detail of the PSI pattern of storm C (elevation angle 4°), when the vortex configuration first appeared in the 1–2 km height level. On some occasions the indicated vortex encircled an echo-free hole. Storm D also displayed a vortex-type PSI pattern around an echo-free hole which at times extended well above 4 km, for about half an hour before 2-inch hailstones fell on the ground; see, for example, Fig. 9 (elevation 9°) showing a hole at 3.5 km. A careful tracing of the arc continuity across the hole, especially in its southern part, reveals an arc pattern which moves toward the radar with clockwise change of azimuth, suggesting cyclonic vorticity in the vicinity of the hole. Note also the very thick arcs near the hole, possibly indicating hazardous turbulence.

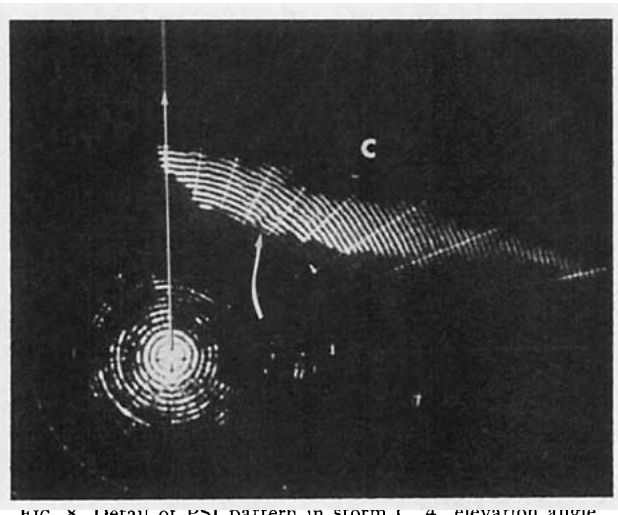

FIG. 8. Detail of PSI pattern in storm C, 4° elevation angle, 1411 EST. Arrow points to characteristic cyclonic vortex pattern, similar to the sketch in Fig. 4.

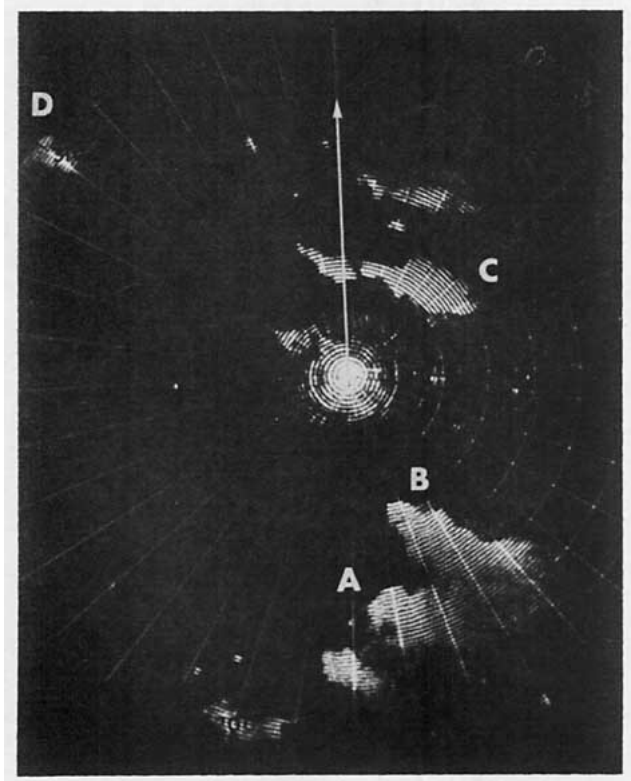

FIG. 7. PSI pattern in storms A, B, C and D at 2° elevation angle, 1357 EST, a few minutes before outbreak of tornado and severe wind damage.

A striking contrast between the shear in two echoes is provided by Fig. 10, taken at 22° elevation. The echo to the south, extending up to about 9 km in height, shows very little if any shear in its PSI pattern. Storm D north of the radar, on the other hand, with a top at about 13 km, has a very disturbed PSI pattern over much of its area, indicative of strong shear. If a Doppler radar with PSI display were available to an aircraft controller at a terminal, aircraft could be warned against entering the northern echo which would very likely be uncomfortable, if not dangerous, to penetrate.

In summary, two operational applications of the PSI display are suggested by the observations of the severe storms of 9 August 1968. First, the appearance of strong wind shear aloft may provide warnings of 15 min or more of the occurrence of large hail and tornadoes or other damaging winds at the ground. Of course, many more cases must be studied to define the limits of reliability of this method for warning of severe thunderstorm hazards. The second application is real-time identification of storms, or portions of storms, in which strong wind shear and turbulence would adversely affect the safety of penetrating aircraft.

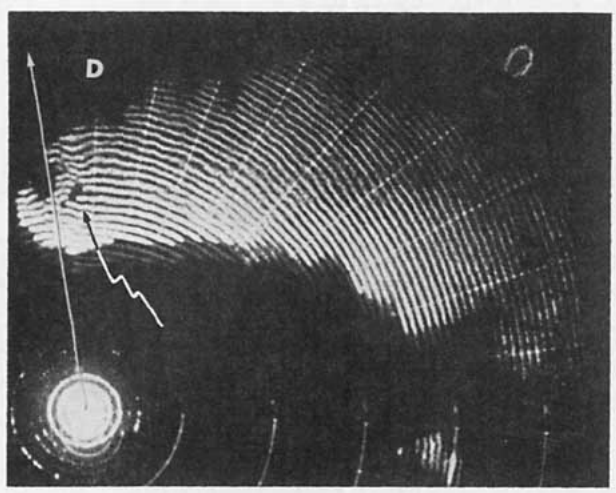

FIG. 9. Detail of PSI pattern in storm D, 9° elevation angle, 1607 EST. Arrow points to echo hole around which the arcs curve in a manner suggestive of cyclonic vorticity.

5. Application of the PSI technique to airborne radar

The Plan Shear Indicator may find useful application as an airborne aid for avoidance of the most turbulent regions in storms. The operational advantage of this improvement to airborne radar may, in certain applications, be worth the additional cost and weight penalty of the necessary Doppler and signal processing capability. For example, pilots of subsonic transports may desire increased assurance of passenger comfort and safety during penetration of clouds outside the range of terminal-based radar control.

Airborne display of PSI data would be most useful in providing information on wind shear within a relatively narrow sector centered around the aircraft heading. The component of wind observed in this manner would be directed along the length of the aircraft, probably the least troublesome vector for affecting aircraft performance. However, airflow continuity in an essentially incompressible atmosphere requires that a strong shear vector in one direction be compensated by comparable magnitudes of shear in the plane normal to this direction. Therefore, observation of intense wind shear along the aircraft heading is an indication of the more dangerous lateral shear components in the same location.

A complete azimuthal scan of the Doppler radar antenna from a rapidly moving aircraft would be confused by a multiplicity of velocity ambiguities, since aircraft speeds may be an order of magnitude higher than the maximum unambiguous velocity of the radar. This problem can be eliminated, however, by restricting the antenna beam motion to a sufficiently small scan angle on either side of the aircraft heading. If the aircraft speed is a factor s times v_{max}, a trigonometric solution for the antenna scan angle $\pm\beta$ within which the component of aircraft speed varies by no more than v_{max} is

$$\cos\beta = 1 - 1/s. \tag{9}$$

If an airplane speed is 250 m sec^{-1}, and the radar v_{max} is 25 m sec^{-1}, $s=10$ and the solution of (9) shows that the antenna beam must scan within $\pm 26°$ of the aircraft heading. Even with an aircraft speed of 20 v_{max}, the permissible scanning angle is still $\pm 18°$. This restriction is not at all unreasonable for avoidance of dangerous PSI patterns.

It is noteworthy that airborne Doppler radar cannot measure wind speeds directly in precipitation or detectable clouds, because the maximum unambiguous velocity of the radar relative to the air is exceeded by an unknown multiple. However, by working within the limitations specified by (9), wind shear components may be determined from an aircraft with no more difficulty than the comparable ground-based radar measurement. After all, it is wind variability or shear, not the magnitude of the wind, which gives the bumpy ride.

Acknowledgments. We are especially grateful for this opportunity to express our appreciation to Dr. Kenneth R. Hardy, Chief, Weather Radar Branch of the Meteorology Laboratory of AFCRL. Dr. Hardy's encouragement of the development of the Plan Shear Indicator and his many valuable suggestions offered during the

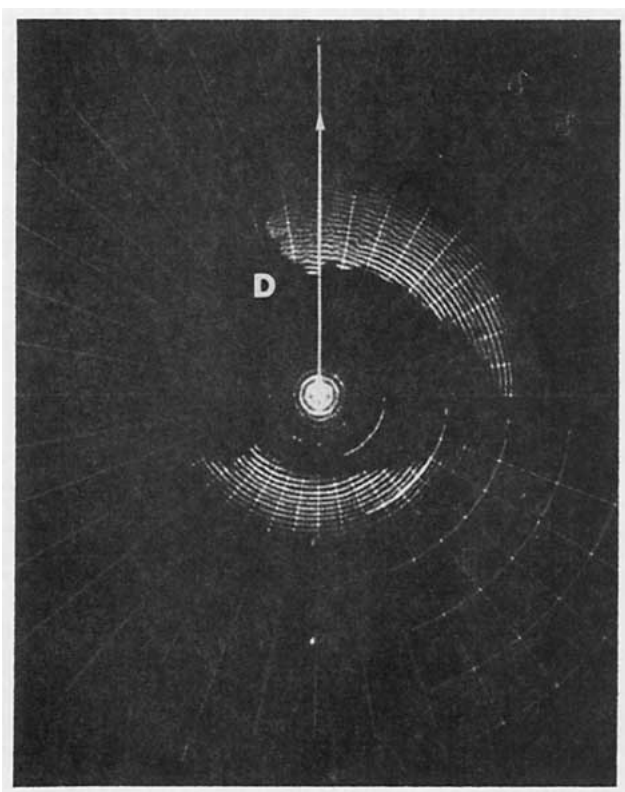

FIG. 10. Contrast in PSI pattern of storm D, north of radar, and anvil of another storm south of radar. Elevation angle 22°, time 1551 EST.

course of our study were vital contributions to this work. We are pleased to acknowledge assistance from other members of the Weather Radar Branch, particularly Mr. Albert C. Chmela and Mr. Michael J. Kraus for their alert, competent job of data acquisition. We also thank Dr. Morton L. Barad, Director, Meteorology Laboratory, for his helpful criticism of our manuscript.

REFERENCES

Armstrong, G. M., and R. J. Donaldson, Jr., 1968: A convenient indicator of tangential shear in radial velocity. *Proc. 13th Radar Meteorology Conf.*, Amer. Meteor. Soc., 50–53. (In this paper "PVI" was erroneously used in place of the more appropriate "PSI.")

Atlas, D., 1963: Radar analysis of severe storms. *Meteor. Monog.*, **5**, No. 27, 177–220.

Bickel, H., E. Brookner, M. Weiss and R. Vogel, 1959: Performance characteristics of the coherent memory filter. *Proc. Fifth Annual Radar Symposium*, Univ. Michigan.

Chimera, A. J., 1960: Meteorological radar echo study. Final Rept. (Appendix C), Contract No. AF 33(616)-6352, Cornell Aero. Labs., Buffalo, N. Y.

Donaldson, R. J., Jr., and R. Wexler, 1969: Flight hazards in thunderstorms determined by Doppler velocity variance. *J. Appl. Meteor.*, **7**, 128–133.

Groginsky, H. L., 1965: The coherent memory filter. *Electron. Progr. (Raytheon Co.)*, **9**, No. 3, 7–13.

Lhermitte, R. M., 1964: Doppler radars as severe storm sensors. *Bull. Amer. Meteor. Soc.*, **45**, 587–596.

Smith, R. L., and D. W. Holmes, 1961: Use of Doppler radar in meteorological observations. *Mon. Wea. Rev.*, **89**, 1–7.